Journal of Applied Polymer Science

Kinetics modeling of carbon-fiber-reinforced bismaleimide composites under microwave and thermal curing

Nanya Li, Yingguang Li, Linglin Zhang, Xiaozhong Hao
College of Mechanical and Electrical Engineering, Nanjing University of Aeronautics and Astronautics, Nanjing, 210016, China

ABSTRACT: This article focuses on the analysis of the curing kinetics of carbon-fiber-reinforced bismaleimide (BMI) composites during microwave (MW) curing. A nonisothermal differential scanning calorimetry (DSC) method was used to obtain an accurate kinetic model. The degree of curing, chemical characterization, and glass-transition temperature of the resin and composites cured by thermal and MW heating were analyzed with DSC, Fourier transform infrared spectroscopy, and dynamic mechanical analysis. The experimental results indicate that MW accelerated the crosslinking reaction of the BMI resin and had different effects on the reaction processes, especially for the glass-transition temperature and chemical bonds. However, the curing reaction rate of the BMI resin decreased when the carbon fibers were added to the BMI resin during thermal and MW curing. According to the experimental results, the curing kinetic model of the BMI composite was used to provide a theoretical foundation for MW curing analysis. © 2016 Wiley Periodicals, Inc. J. Appl. Polym. Sci. **2016**, *133*, 43770.

KEYWORDS: composites; crosslinking; irradiation; kinetics

Received 22 September 2015; accepted 5 April 2016
DOI: 10.1002/app.43770

INTRODUCTION

Carbon-fiber-reinforced bismaleimide (BMI) composites have higher operating temperatures, better damage tolerance, and longer fatigue lives than epoxy composites. Autoclave processing technologies are usually applied to manufacture this kind of composite material, but the extremely long curing cycle and high cost restrict its development. Out-of-autoclave curing approaches, such as microwave (MW) heating, can dramatically reduce these problems.[1,2] The composite manufacturing industries have already attempted to use MW curing technologies to manufacture high-performance composites,[3,4] whereas the MW curing kinetics of carbon-fiber-reinforced BMI composites still remains unclear.

MW curing technologies offer advantages over thermal curing; these include uniform temperature distribution and low temperature gradient and energy consumption.[5] The experimental results of Chaowasakoo and Sombatsompop[6] and Sgriccia and Hawley[7] indicate that MW-heated composite samples had shorter curing times and higher strengths. Navabpour *et al.*[8] showed that bisphenol A (diglycidyl ether of bisphenol A) with an amine–phenol accelerator agent had different activation energies for conventional and MW curing and suggested that different reaction mechanisms were responsible for curing with the two heating methods. Adnadjevic and Jovanovic[9] showed that the formation time of a poly(acrylic acid) hydrogel was decreased with 2.45 GHz of MW radiation. Even for different curing agents applied during epoxy curing,[10] MW heating also accelerated the curing process.[11] The thermophysical properties of MW-cured carbon fiber/epoxy resin composites were studied by Rao and Rao.[12] Vergara *et al.*[13] and Jacob *et al.*[14] discussed the MW and conventional curing processes; their experimental results show that the curing rate of resins cured by MWs was faster than thermal curing. Komorowska-Durka *et al.*[15] reviewed the effects of polycondensation reactions of polymer resins during MW processes with no curing reaction mechanism explanations. Zainol *et al.*[16] compared the thermal and MW curing of BMI resin; the results show that the BMI resin was cured faster in the MW oven and showed no difference in the chemical reaction taking place during MW and thermal curing. Papargyris *et al.*[17] found that MW-cured carbon fiber/epoxy composites exhibited 130 °C glass-transition temperatures and conventional cured composites exhibited 128 °C glass-transition temperatures.

As mentioned previously, MW and thermal curing of polymer resins exhibit different heating mechanisms. It is necessary to conduct a fundamental reaction study of the MW curing process to elucidate the basic design foundation of the MW curing process parameters and to contribute to the improvement of the final product performance and quality. These reaction kinetics can also be used to calculate the degree of curing and the exothermal reaction heat of a finite element model to predict the temperature distribution of the composite during MW curing, particularly in the aerospace industry. To analyze the

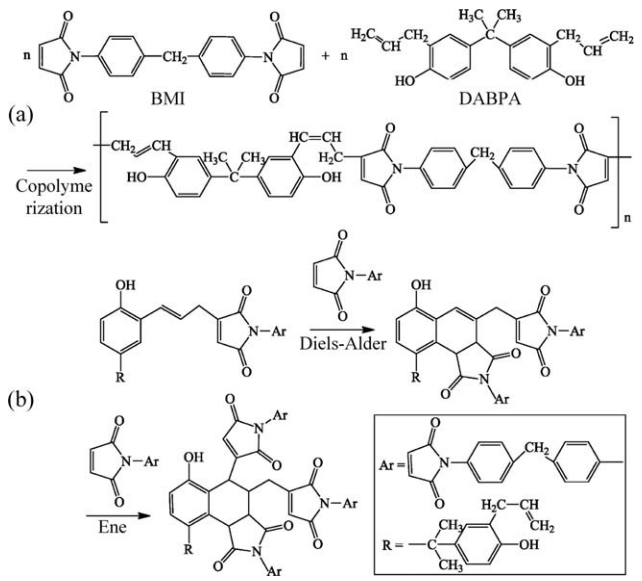

Figure 1. Chemical reactions occurring between BMI and DABPA: (a) copolymerization reaction and (b) Diels–Alder and ene reactions.

curing kinetics of carbon-fiber-reinforced BMI composites under MW and thermal curing, comparative experiments were implemented in this study. Nonisothermal differential scanning, Fourier transform infrared (FTIR) spectroscopy, and dynamic mechanical analyzing were used to characterize the curing kinetic process of MW curing. The crosslinking reaction rates, activation energies, change in chemical bonds, and glass-transition temperatures of BMI resins with or without carbon fibers were analyzed.

EXPERIMENTAL

Materials

T300 carbon fiber (Toray Industries, Inc.) and BMI resin (Beijing Aeronautical Manufacturing Technology Research Institute) were used in this experiment. The curing agent was diallyl bisphenol A (DABPA). The carbon fiber and BMI resin were impregnated into the prepreg, and the carbon-fiber volume content was 66%. The prepreg thickness was 0.125 mm, and the fiber areal weight was 125 g/m^2. Three samples were tested in each measurement, and the average values were applied in this research.

Nonisothermal Curing Kinetics Approaches

The reaction process of BMI curing has been reported extensively in the literature.[18,19] Because the crosslinking of BMI resin and DABPA generally shows two curing exothermic peaks, this phenomenon suggested that two different reactions occur during curing process, as shown in Figure 1. The copolymerization of BMI and DABPA occurred first, and DABPA increased the length of the copolymer chains to improve the toughness, as shown in Figure 1(a). As the curing temperature increased, the Diels–Alder and ene reactions responsible for the reaction of the C═C double bond between molecules took place, and the three-dimensional network of the BMI resin was built, as shown in Figure 1(b).

The nonisothermal curing kinetics of a matrix resin was characterized with differential scanning calorimetry (DSC).[20–22] The curing kinetics of the conventionally thermally cured BMI resin was monitored on site with a Netzsch DSC 204F1 instrument. However, to measure the reaction exotherm of the MW-cured resin, the samples are heated in a MW chamber[23] to some interval points of whole curing at different heating rates (βs). Then, the remaining reaction exotherms of the samples at different interval points were tested with DSC. The reaction exotherm derived from DSC measurement was the measured quantity used to describe the heat of the reaction. As the BMI resin started to react from 403 K, the measuring stage of the MW-cured samples was from 403 to 553 K. FTIR spectroscopy (ThermoFisher Nicolet iS10) was introduced to measure the content of different functional groups in the thermal and MW processes. The FTIR measurement was carried out at a 4-cm^{-1} resolution. Spectra were scanned from 500 to 4000 cm^{-1} at 293 K. The degree of conversion (α) of the composite samples was evaluated as follows[24]:

$$\alpha = \frac{\Delta H}{H_{\text{total}}} \tag{1}$$

where ΔH is the reaction exotherm at a certain curing temperature and H_{total} is the total reaction exotherm. To calculate the degrees of curing of the MW-cured composite samples, the most widely used kinetic method for cured resin systems was used[25]:

$$\frac{d\alpha}{dt} = \beta \frac{d\alpha}{dT} = k(T) f(\alpha) \tag{2}$$

where $\beta = dT/dt$, $k(T)$ is the reaction rate constant, $f(\alpha)$ is the reaction model, and $d\alpha/dt$ is the rate of conversion. $k(T)$ only depends on the temperature, which can be obtained according to the Arrhenius law:

$$k(T) = A \exp\left(-\frac{E}{RT}\right) \tag{3}$$

where A is the frequency factor, E is the activation energy, R is the universal gas constant, and T is the curing temperature. According to eqs. (2) and (3), the isoconversional method of Friedmann obeys the expression[26]

$$\ln[\beta(d\alpha/dT)] = \ln[Af(\alpha)] - E/RT \tag{4}$$

The plot of $\ln(d\alpha/dt)$ versus $1/T$ yields the apparent E. According to the Friedman method, E is related to the curing degree, but the difference is negligible within a range of 0.15–0.85 of

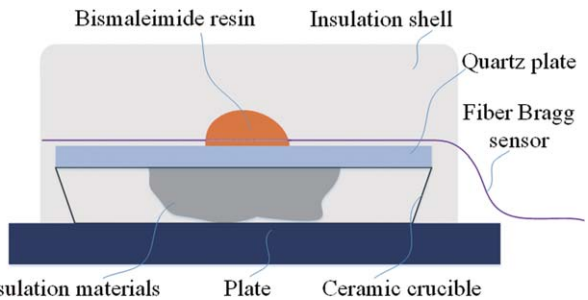

Figure 2. Schematic of the MW curing process. [Color figure can be viewed in the online issue, which is available at wileyonlinelibrary.com.]

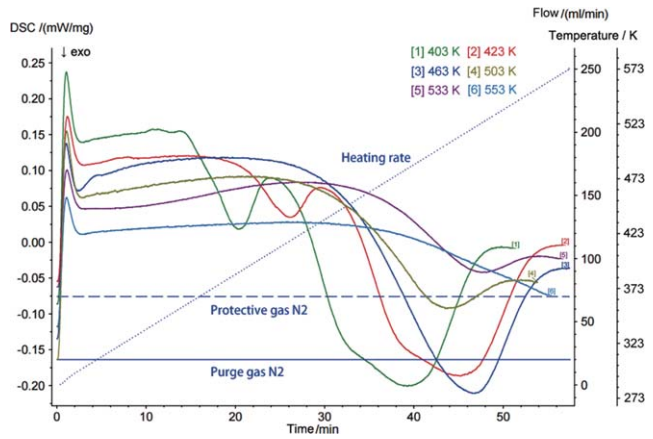

Figure 3. DSC results for the MW-cured BMI resin samples at 5 K/min. [Color figure can be viewed in the online issue, which is available at wileyonlinelibrary.com.]

the curing degree. Thus, it was reasonable to use the mean E value in the following calculation. The kinetics of the autocatalytic polymerization reaction model are represented with the following equation[27]:

$$\frac{d\alpha}{dt}=(k_1+k_2\alpha^m)(1-\alpha^n)=k(B+\alpha^m)(1-\alpha)^n \quad (5)$$

where k_1 is the noncatalytic polymerization reaction rate constant, k_2 is the autocatalytic polymerization reaction rate constant, B is a temperature-independent parameter when the values of k_1 and k_2 are equal, and m and n are the orders of the autocatalytic and noncatalyzed polymerization reactions, respectively. Because the value of k_1 is much lower than that of k_2, B is assumed to be constant. This autocatalytic reaction model has been widely applied to represent the curing kinetics of BMI resins.[28]

Equation (5) has different mechanistic-like meanings when different values are assigned to m and n. According to a semiempirical velocity equation, the case $m=1$ directly related to this study. Thus, eq. (5) can be expressed as follows:

$$\frac{d\alpha}{dt}=A\exp\left(-\frac{E}{RT}\right)(B+\alpha)(1-\alpha)^n \quad (6)$$

The inflection point of the $d\alpha/dt$ curve at the maximum point is zero. On the basis of eq. (6), B can be expressed as follows:

$$B=\frac{1}{n/1-\alpha_p-E/RT_p^2(d\alpha/dt)_p}-\alpha_p \quad (7)$$

where $(d\alpha/dt)_p$, α_p, and T_p represent the values of $d\alpha/dt$, α, and T at the inflection points of different curves, respectively. Several representative βs, including 2, 5, and 10 K/min, were used to characterize the curing kinetics in this experiment.

MW Curing Techniques and Dynamic Mechanical Analysis

MW heating takes place through strong interactions between polar molecules and electromagnetic waves; a fast and direct curing is realized rather than the slow thermal conduction and indirect heating that occurs in the conventional thermal process. A 20-kW MW curing oven (2.45 GHz) with an octahedron chamber was used,[22] and the schematic of the MW curing process is shown in Figure 2. The BMI resin was placed on a quartz plate, and the temperature measurement section of a Fiber Bragg Grating (FBG) sensor was buried in the resin. Insulation

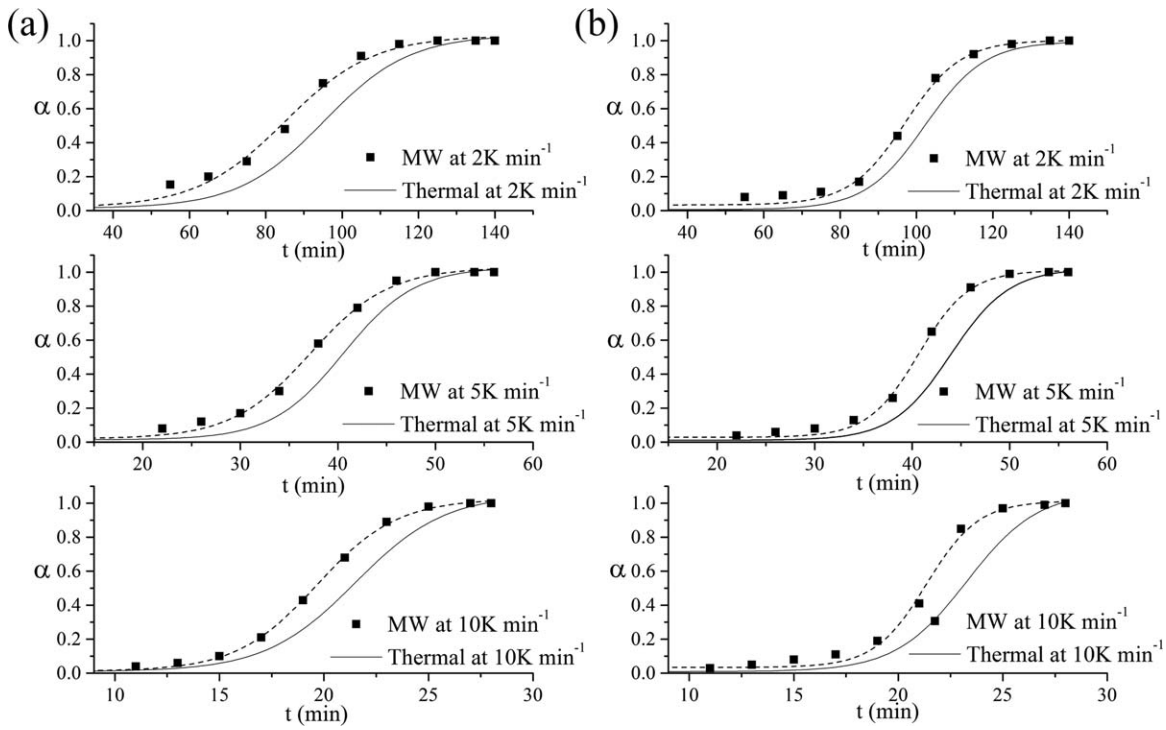

Figure 4. Degree of curing of the BMI resin and prepreg cured by thermal and MW curing at different βs: (a) prepreg cured by the thermal and MW processes and (b) BMI resin cured by the thermal and MW processes.

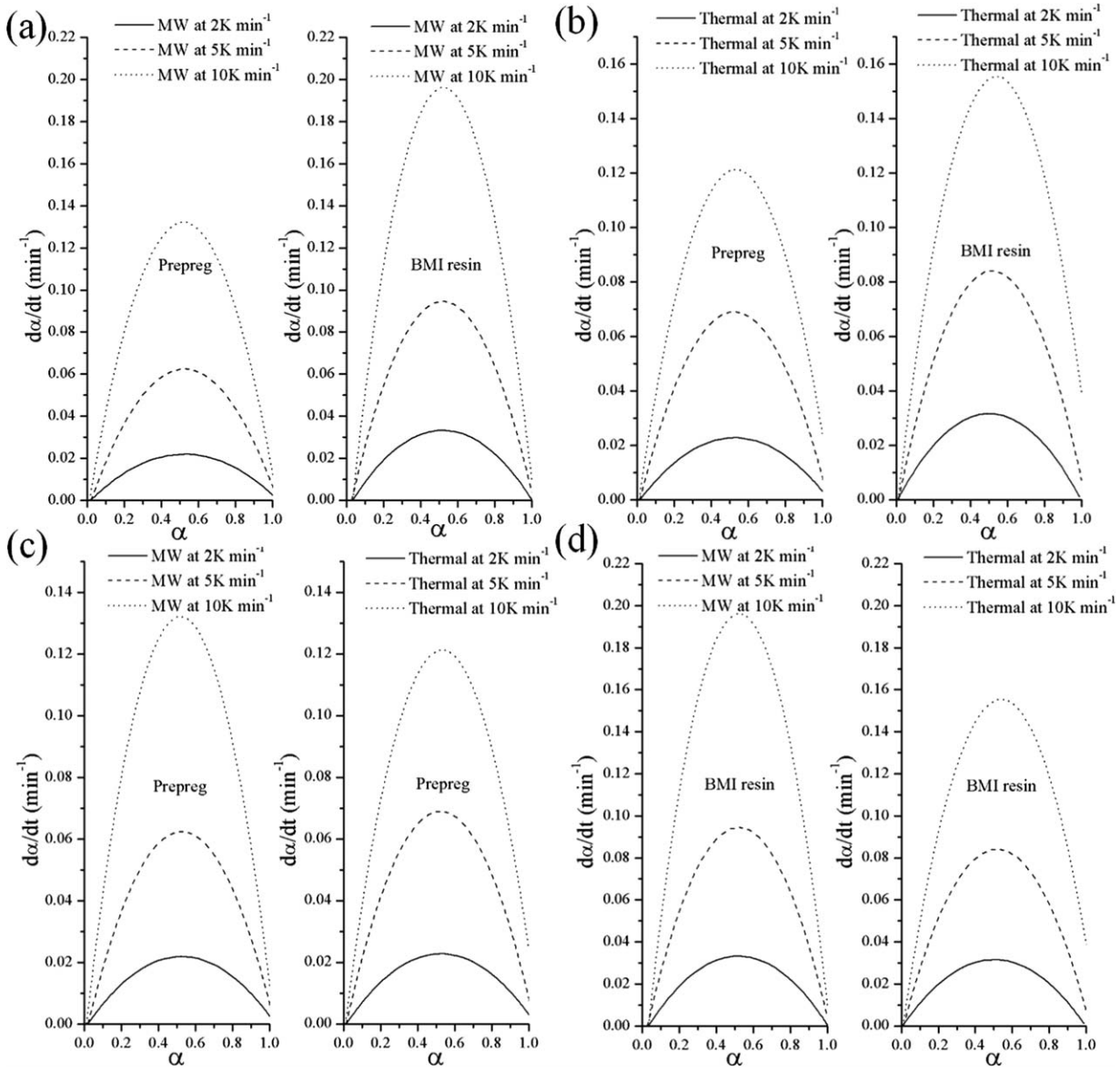

Figure 5. Relationship of the degree of curing of the BMI resin and carbon-fiber mixed resin cured by conventional and MW curing at different βs: (a) prepreg and BMI resin cured by MW heating, (b) prepreg and BMI resin cured by thermal heating, (c) prepreg cured by MW and thermal heating, and (d) BMI resin cured by MW and thermal heating.

materials were used to prevent heat loss, and the temperature around the resin material was still room temperature. The heating temperature was demodulated from optical signals with an MS125 interrogating system. To evaluate the permittivity of the carbon fiber and BMI resin, coaxial line measurement methods (Agilent N5230A) were used.

A Hitachi DMS 6100 dynamic mechanical analyzer was used to characterize the glass-transition temperature of the MW and thermally cured composite samples. The size of the sample was 35 mm long, 10 mm wide, and 3 mm thick, and the storage modulus (E') and loss tangent (tan δ) were evaluated by a single-cantilever tool. The tests were performed with six different samples at a frequency of 1 Hz and an amplitude of 50 μm. The temperature range was 293 to 623 K at a β of 5 K/min.

RESULTS AND DISCUSSION

Curing Degree of Nonisothermal Heating

The nonisothermal curing degree of the conventional and MW heating of the composite samples were monitored by the application of the DSC method. For the traditional thermally cured samples, the reaction exotherm heat was directly measured by DSC and calculated as the curing degree on the basis of eq. (1). However, the curing degrees of the samples cured by MWs were obtained by the measurement of the remaining heats of reaction of the samples cured by MWs at different temperature intervals. The differential scanning results of the reaction exotherm of the MW-cured BMI resin samples were measured from 403 to 573 K at a β of 5 K/min, as shown in Figure 3. Both the protective gas and purge gas were nitrogen, and the flow rates were

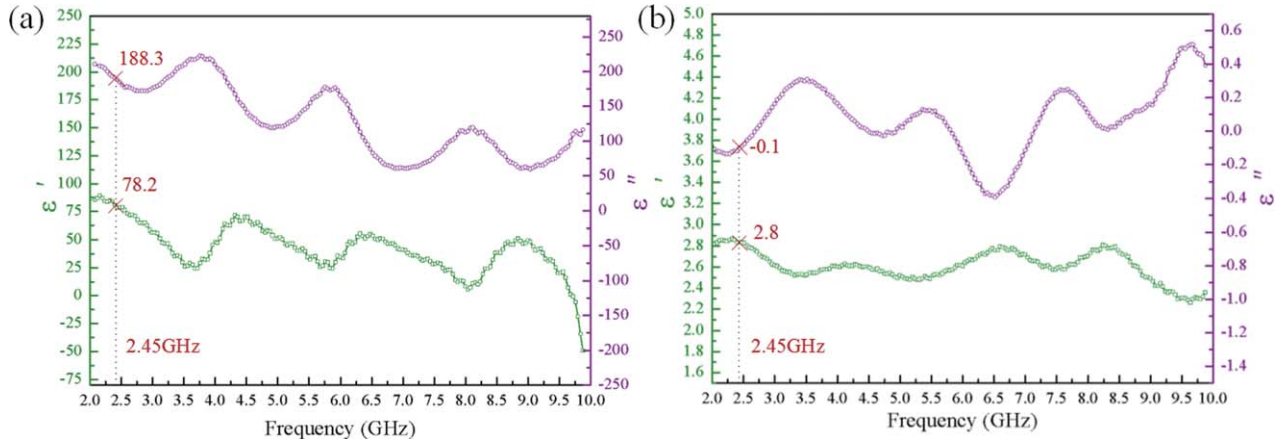

Figure 6. Complex permittivity versus frequency: (a) real and imaginary parts of the permittivity of the carbon fiber and (b) permittivity of the BMI resin. [Color figure can be viewed in the online issue, which is available at wileyonlinelibrary.com.]

70 and 20 mL/min, respectively. The DSC curve at 403 K indicated that the crosslinking reaction did not occur after the MW heating of the sample to 403 K. Also, the two exothermic peaks showed that two different reactions occurred sequentially. The exothermic values of the resin samples decreased as with the increase in MW heating temperature.

According to the curing degree of the BMI resin and carbon-fiber-added resin (prepreg) samples cured by thermal and MW curing, the relationship of the curing degree and time is shown in Figure 4. All of the MW-cured samples exhibited a higher curing degree at the same time than the thermally cured ones. The total time required for MW irradiation to achieve the maximum degree of curing of the composite was about 140 min at a β of 2 K/min. As shown in Figure 4, MW heating technology improved the curing rate compared with conventional thermal heating at three different βs. Therefore, the MW energy had a positive effect on the cuing process of the BMI resin and prepreg.

The relationship of $d\alpha/dt$ and the degree of curing of the BMI resin and prepreg cured by thermal and MW heating at different βs is shown in Figure 5. The dependence of the process rate on the temperature of the four curves were cross-compared to represent the MW effect on samples with or without carbon fibers. For the MW-cured samples, the reaction rates decreased obviously as carbon fibers were introduced at three different βs, as shown in Figure 5(a). This implied that the curing reaction rate of the BMI resin decreased when the carbon fibers mixed in the BMI resin. The permittivity of the carbon fiber and BMI resin were measured to explain the mechanism, as shown in Figure 6, where ε′ and ε″ are the real part and imaginary part of complex dielectric constant, respectively. Because the MW energy absorption rate is defined by the dielectric tan δ of the material, the dielectric tan δ values of the carbon fibers and BMI resin were calculated through ε″/ε′. The average dielectric tan δ of the carbon fiber and BMI resin were about 2.6 and 0.03, respectively. We observed that the MW energy was nearly all absorbed by the carbon fibers, as shown by the extremely high dielectric tan δ of the carbon fiber compared with that of the BMI resin. Thus, the accelerating effect of MW curing for the crosslinking reaction of the BMI resin was eliminated. On the other side, the high volume fraction of the carbon fibers increased the distance between the molecular chain and raised the difficulty of the curing reaction. However, for the thermal curing process, the carbon fiber and resin were simultaneously heated, and only the second reason discussed previously affected the reaction rate of the BMI resin. The results are shown in Figure 5(b). The thermally cured samples possessed the same variation tendency of MW heating, but the difference between the BMI resin and prepreg was smaller than that of MW heating. As shown in Figure 5(c), the MW-cured samples had a higher reaction rate at 10 K/min than the thermally cured ones, but the opposite conditions appeared at 2 and 5 K/min. Those

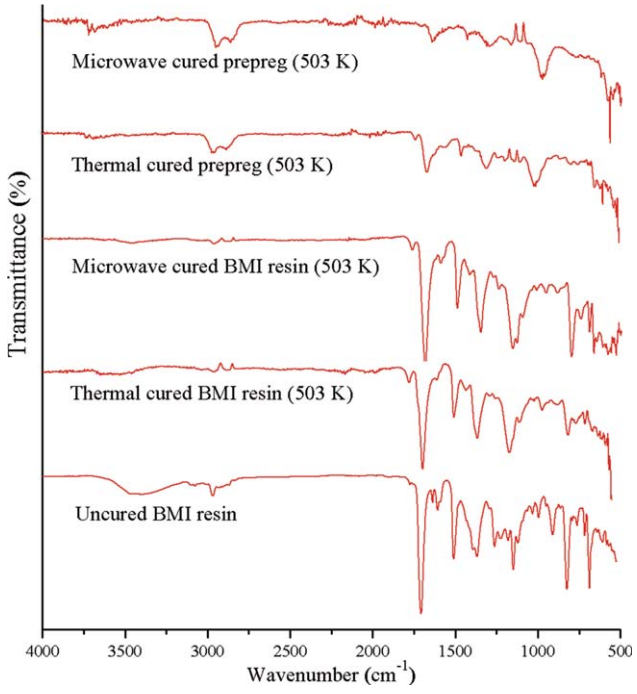

Figure 7. FTIR spectra of the uncured BMI resin and MW-cured and thermally cured samples at 503 K. [Color figure can be viewed in the online issue, which is available at wileyonlinelibrary.com.]

Table I. Statistical Analysis of the FTIR Spectra of Different Samples

	Peak height at 2970 cm^{-1} (%)	Peak height at 820 cm^{-1} (%)	Peak height at 687 cm^{-1} (%)
Uncured BMI resin	8.04	61.38	54.97
BMI resin at 503 K (thermal)	3.95	51.48	25.08
BMI resin at 503 K (MW)	1.45	25.62	14.02
Prepreg at 503 K (thermal)	4.99	41.29	37.29
Prepreg at 503 K (MW)	3.62	41.25	38.32

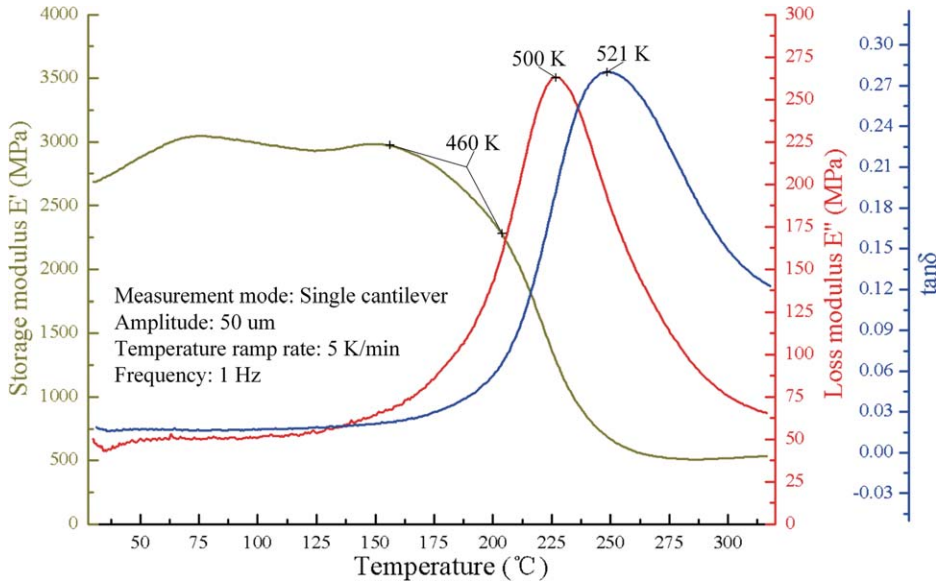

Figure 8. Dynamic mechanical analysis measurement results for thermally cured samples. [Color figure can be viewed in the online issue, which is available at wileyonlinelibrary.com.]

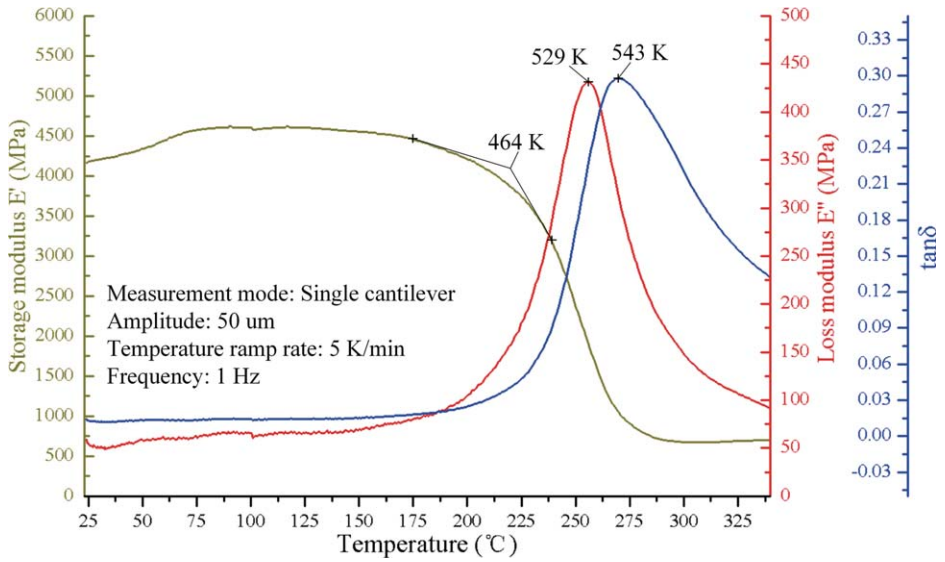

Figure 9. Dynamic mechanical analysis measurement results for the MW-cured samples. [Color figure can be viewed in the online issue, which is available at wileyonlinelibrary.com.]

Table II. Kinetic Parameters of Different Samples

Sample	*E* (kJ/mol)	*A*	*B*	*n*
Prepreg: MW	88.61	2.97×10^{9}	0.2326	2.588
Prepreg: thermal	115.81	6.88×10^{11}	0.7079	2.745
Resin: MW	101.95	5.63×10^{10}	0.0749	2.119
Resin: thermal	114.19	2.72×10^{11}	0.1983	2.312

might have been caused by the sizing agent on the surface of the carbon fiber with multiple reaction-active groups. At high β, the carbon fiber received more MW energy and owned a higher temperature than the BMI resin. Thus, the reaction between the sizing agent and BMI resin on the interface of the fiber and resin was promoted. Figure 5(d) shows the reaction rate of the BMI resin processed by MW and thermal heating and indicates that, apparently, MW heating accelerated the crosslinking reaction of the BMI resin.

Chemical Characterization

To characterize the differences in the chemical bonds of the prepreg and BMI resin cured by MW and thermal heating, FTIR spectra of the samples heated at 5 K/min were obtained, as shown in Figure 7. The samples were scanned from 500 to 4000 cm^{-1}. The peak height between 1698 and 1707 cm^{-1}, which was attributable to the C═O bonds, was used to demarcate the peak heights of the other chemical bonds.[29] Through analysis of the variation tendency of the curves in Figure 7, there was no difference in the chemical reactions mechanism during MW and thermal curing. The quantitative analysis of the methylene bonds (2970 cm^{-1}) and carbon–carbon double bonds (820 and 687 cm^{-1}) was implemented to determine the reaction rates of different curing approaches, and the results are shown in Table I. The contents of methylene bonds (—CH_2—) and carbon–carbon double bonds (C═C) of the uncured BMI resin were higher than those of the cured samples. This indicated that the methylene bonds and carbon–carbon double bonds were consumed during the curing reaction. As shown in Table I, the height values of three peaks of the MW-cured BMI resins were lower than those of the thermally cured ones at 503 K. Therefore, more chemical bonds were consumed in the MW-cured samples, and this indicated that MW heating was able to accelerate the reaction process of the BMI resin. However, for the MW and thermally cured prepreg samples, the contents of methylene bonds and carbon–carbon double bonds were almost the same. This interesting result also showed that the existence of carbon fiber impeded the acceleration phenomenon of MW curing.

By comparing the peak height at 2970, 820, and 687 cm^{-1} of the MW and thermally cured BMI resins, we found that the consumption rate of the MW-cured sample at 2970 cm^{-1} was higher than that of the thermally cured sample by 61%. For the IR spectrum at 820 and 687 cm^{-1}, the consumption rate of the MW-cured sample was higher than that of the thermally cured sample by 261 and 37%, respectively. This showed that for different chemical bonds, MW curing had different accelerative effects on the reaction process, and this may have been relate to the polarity of the molecules.

Glass-Transition Temperature and Curing Kinetics Modeling

To accurately describe the differences in the glass-transition temperature values of the two kinds of curing methods, the E' and tan δ values of the MW and thermally cured samples were measured (three samples from each group). We calculated the values marked in Figures 8 and 9 by taking the average of three samples. The glass-transition temperatures of different samples are shown in Figures 8 and 9. As shown in Figure 8, the turning and peak points of E' and tan δ of the thermally cured samples were 460 and 521 K, respectively. Those values indicate that the starting temperature and terminating glass-transition temperature of the thermally cured samples. As shown in Figure 9, the MW-cured samples had higher starting and terminating glass-transition temperatures than the conventionally thermally cured samples. The peak temperature of the tan δ curve of the MW-cured sample was higher than that of the thermally cured one at about 22 K. A significant increase in E' of the composites via MW curing was observed as well. This phenomenon could be explained as the improved interfacial strength between the carbon fiber and resin because the high temperature of the carbon fiber caused a preferential crosslinking reaction on the interface during MW curing.

According to eq. (6), the parameters of *E*, like k_0, *n*, and *B*, were calculated statistically by the numerical fitting of $d\alpha/dt$ at different βs, as shown in Table II. Through comparative analysis of the reaction *E*s of the MW and thermal curing processes, the lower activation of the MW curing energy was observed. Thus, the crosslinking reaction of the BMI resin during MW heating proceeded more easily. On the basis of the results shown in Table II, the reaction model of the carbon-fiber-reinforced BMI composites under MW curing could be obtained as follows:

$$\frac{d\alpha}{dt}=2.97\times10^{9}\exp\left(-\frac{88.61\times10^{3}}{RT}\right)(0.2326+\alpha)(1-\alpha)^{2.588} \quad (8)$$

Other reaction equations could also be established on the basis of the parameters shown in Table II. The equation of thermal curing had good fitting with $d\alpha/dt$ at different βs. However, for MW curing, the curves provided better fitting at higher βs (>2 K/min) because of the poor temperature control of MW heating at low βs. Also, one can acquire accurate equations through the iterative correction of those parameters, which are capable of providing curing kinetic models for MW curing temperature predictions in the aerospace industry.

CONCLUSIONS

Through quantitative and statistical research, the reaction rate of MW curing was shown to be significantly higher than that of thermal heating for both the prepreg and BMI resin samples. Higher levels of curing (as judged by FTIR spectroscopy monitoring of chemical bond consumption) of the BMI resin cured by MW than compared to that cured thermally was exhibited. For different chemical bonds, MW curing showed different accelerative effects on the reaction processes; this may have been related to the polarity of the molecules. Through a comparison of the glass-transition temperature of the samples measured by dynamic mechanical analysis, the glass-transition temperatures of the MW-cured samples were higher than those of the thermally cured ones for about 22 K. This could be explained as an improvement of the interfacial strength between the carbon fiber and resin during MW curing. Finally, *E* and the MW curing kinetic models of the carbon-fiber-reinforced BMI composite were calculated to elucidate the basic design foundation of the MW curing process and to contribute to the improvement of the final product performance and quality.

ACKNOWLEDGMENTS

This project was supported by the National Natural Science Foundation of China (contract grant numbers 51575275 and 51305195) and was jointly supported by the Outstanding Talents Cultivation Fund (contract grant number NE2012003), the Major Breeding Project (contract grant number NP2014201), and the Funding of Jiangsu Innovation Program for Graduate Education of the Nanjing University of Aeronautics and Astronautics (contract grant number KYLX_0310).

REFERENCES

1. Adeolu, A.; Daniyan, I.; Azeez, T.; Omohimoria, C. *Adv. Mater.* **2015**, *4*, 67.
2. Li, Y.; Li, N.; Gao, J. *Int. J. Adv. Manuf. Technol.* **2014**, *70*, 591.
3. Feher, L. E.; Thumm, M. K. *IEEE Trans. Plasma Sci.* **2004**, *32*, 73.
4. Li, N.; Li, Y.; Hang, X.; Gao, J. *J. Mater. Process. Technol.* **2014**, *214*, 544.
5. Tanrattanakul, V.; Jaroendee, D. *J. Appl. Polym. Sci.* **2006**, *102*, 1059.
6. Chaowasakoo, T.; Sombatsompop, N. *Compos. Sci. Technol.* **2007**, *67*, 2282.
7. Sgriccia, N.; Hawley, M. *Compos. Sci. Technol.* **2007**, *67*, 1986.
8. Navabpour, P.; Nesbitt, A.; Mann, T.; Day, R. J. *J. Appl. Polym. Sci.* **2007**, *104*, 2054.
9. Adnadjevic, B.; Jovanovic, J. Advances in Induction and Microwave Heating of Mineral and Organic Materials; InTech Open Access: Rijeka, Croatia, **2011**; Chapter 18, p 395.
10. Boey, F.; Yap, B.; Chia, L. *Polym. Test.* **1999**, *18*, 93.
11. Shimamoto, D.; Yusuke Imai, Y. H. *J. Compos. Mater.* **2014**, *4*, 85.
12. Rao, S.; Rao, R. *Polym. Test.* **2008**, *27*, 645.
13. Lopez de Vergara, U.; Sarrionandia, M.; Gondra, K.; Aurrekoetxea, J. *Thermochim. Acta* **2014**, *581*, 92.
14. Jacob, J.; Chia, L.; Boey, F. *J. Mater. Sci.* **1995**, *30*, 5321.
15. Komorowska-Durka, M.; Dimitrakis, G.; Bogdał, D.; Stankiewicz, A. I.; Stefanidis, G. D. *Chem. Eng. J.* **2015**, *264*, 633.
16. Zainol, I.; Day, R.; Heatley, F. *J. Appl. Polym. Sci.* **2003**, *90*, 2764.
17. Papargyris, D. A.; Day, R. J.; Nesbitt, A.; Bakavos, D. *Compos. Sci. Technol.* **2008**, *68*, 1854.
18. Boey, F.; Song, X.; Rath, S.; Yue, C. *J. Appl. Polym. Sci.* **2002**, *85*, 227.
19. Frigione, M.; Kenny, J. *Adv. Polym. Technol.* **2005**, *24*, 253.
20. Hedreul, C.; Galy, J.; Dupuy, J.; Delmotte, M.; More, C. *J. Appl. Polym. Sci.* **1998**, *68*, 543.
21. Sun, H.; Liu, Y.; Wang, Y.; Tan, H. *J. Appl. Polym. Sci.* **2014**, *131*, 8761.
22. Hao, W.; Hu, J.; Chen, L.; Zhang, J.; Xing, L.; Yang, W. *Polym. Test.* **2011**, *30*, 349.
23. Li, N.; Li, Y.; Hao, X.; Gao, J. *Compos. Sci. Technol.* **2015**, *106*, 15.
24. Garschke, C.; Parlevliet, P.; Weimer, C.; Fox, B. *Polym. Test.* **2013**, *32*, 150.
25. Janković, B. *Thermochim. Acta* **2011**, *519*, 114.
26. Friedman, H. L. *J. Polym. Sci. Part C: Polym. Symp.* **1964**, *6*, 183.
27. Zvetkov, V. *Polymer* **2001**, *42*, 6687.
28. Boey, F. Y.; Song, X.; Yue, C.; Zhao, Q. *J. Polym. Sci. Part A: Polym. Chem.* **2000**, *38*, 907.
29. Chiang, T. H.; Liu, C. Y.; Dai, C. Y. *J. Polym. Res.* **2013**, *20*, 1.